Macromolecules
ARTICLE

Macromolecules **2010**, *43*, 6353–6360 **6353**
DOI: 10.1021/ma101115t

Synthesis of Narrowly Size-Distributed Thermosensitive Poly(*N*-isopropylacrylamide) Nanocapsules in Inverse Miniemulsion

Zhihai Cao,[†] Ulrich Ziener,*[,†] and Katharina Landfester*[,†,‡]

[†]*Institute of Organic Chemistry III − Macromolecular Chemistry and Organic Materials, University of Ulm, Albert-Einstein-Allee 11, 89081 Ulm, Germany, and* [‡]*Max Planck Institute for Polymer Research, Ackermannweg 10, 55128 Mainz, Germany*

Received May 20, 2010; Revised Manuscript Received July 1, 2010

ABSTRACT: Narrowly size-distributed thermosensitive poly(*N*-isopropylacrylamide) (PNIPAM) nanocapsules with a hydrophilic core composed of an aqueous solution of cobalt tetrafluoroborate (CoTFB) were synthesized via a one-pot polymerization of *N*-isopropylacrylamide (NIPAM) and the cross-linking agent *N*,*N*′-methylene bis(acrylamide) (MBA) in inverse miniemulsion. CoTFB not only worked as template and lipophobe, but also promoted the dissolution of NIPAM in water by the formation of a complex between NIPAM and CoTFB. The formation of PNIPAM nanocapsules was verified by transmission electron microscopy (TEM) and atomic force microscopy (AFM). This is the first report to synthesize nanocapsules in inverse miniemulsion by following a phase separation mechanism as proposed by Tiarks et al. in direct miniemulsion [Tiarks, F.; Landfester, K.; Antonietti, M. *Langmuir* **2001**, *17*, 908−918]. The particle size distribution was narrowed by increasing the weight content of CoTFB, MBA, and water. The particle size of the nanocapsules could be conveniently tuned by varying the weight content of CoTFB and MBA. The as-prepared PNIPAM nanocapsules showed reversible thermosensitive properties. An ordered monolayer of PNIPAM nanocapsules could form by controlling the evaporation of apolar solvent, and moreover the size and thus interparticle distance of PNIPAM nanocapsules in the ordered arrays could be tuned by drying the sample under different temperatures below and above the lower critical solution temperature (LCST) of PNIPAM.

Introduction

Capsules have drawn intense attention in the past decades due to their practical and potential applications in a wide range of fields such as drug delivery system, biology, catalysis, cosmetics, and coating by encapsulating drugs, DNA, catalysts, dyes, and so on.[1−4] Capsules with an environmentally stimuli-responsive polymeric shell are of high interest due to the fact that the permeability of the capsules can possibly be tuned by changing the external stimuli, for instance light, pH, ionic strength, temperature, etc., which provides control over loading or release of guest materials from the inner core of the capsules.[5−7]

Among the variety of stimuli-responsive polymers, poly(*N*-isopropylacrylamide) (PNIPAM) is one of the most popular and widely investigated environmentally sensitive polymers since it was first reported by Heskins et al.[8] As temperature increases, PNIPAM can undergo a "coil to globule" volume phase transition near the lower critical solution temperature (LCST, about 32 °C) due to the breakdown of hydrogen bonds between water molecules and amide groups and the release of hydrophobically structured water around the isopropyl groups.[9] The PNIPAM nano/microcapsules can be prepared by using hard or soft templates in various heterogeneous polymerization systems like precipitation, inverse emulsion, or inverse miniemulsion polymerization or layer-by-layer (LbL) assembly technique. Gao et al.[5] prepared fluorescent PNIPAM nanocapsules by forming a cross-linked PNIPAM shell on an isothiocyanate fluorescein (FITC)-trapped silica particle template via precipitation polymerization of *N*-isopropylacrylamide (NIPAM) followed by etching the SiO_2 core by hydrofluoric acid (HF). Recently, an ultrathin thermo-responsive microcapsule was fabricated through direct covalent LbL assembly of azido- and acetylene-functionalized PNIPAM onto azido-modified silica particles using click chemistry followed by the removal of the silica templates.[10] Compared to hard templates, soft templates are more promising with respect to the possibility to directly incorporate guest materials in the core of nanocapsules. With aqueous droplet templates, hollow structured PNIPAM microspheres were prepared via an interfacial polymerization in inverse emulsion as reported by Deng et al.[11] and Horecha et al.[12] The polymerization needs to be carried out above the LCST of PNIPAM to ensure the phase separation of the polymer during the polymerization to form the shell. Deng et al. realized the interfacial polymerization of NIPAM by using a pair of interfacial redox initiators.[11] Horecha et al. used a macromolecular surfactant to act as seeds for selective precipitation of the phase-separated PNIPAM leading to the formation of microcapsules.[12] Miniemulsion polymerization has shown great advantages to synthesize nanocapsules using soft templates (hydrophobic[13−19] or hydrophilic[20−23] liquid core) because of its droplet nucleation mechanism. Recently, Lu et al.[23] reported a method to synthesize PNIPAM nanocapsules via interfacially confined polymerization by using an amphiphilic PEO−RAFT agent in inverse miniemulsion. They predicted that the functionality and thickness of the polymer shell could possibly be controlled via RAFT polymerization. So far, the control of particle size distribution of PNIPAM nanocapsules synthesized by inverse miniemulsion polymerization is still an open question. Our group has aimed to synthesize narrowly size-distributed particles containing metal salts via miniemulsion polymerization.[24−26] Up to now, two kinds of monodisperse water-soluble polymer/metal salt particles, namely poly(2-hydroxyethyl methacrylate)/cobalt tetrafluoroborate and poly(acrylamide)/zinc nitrate, have been successfully synthesized via inverse miniemulsion.[25,26] Compared to the previous papers, besides the morphology of PNIPAM nanocapsules we paid more attention to control the particle size distribution of PNIPAM

*Corresponding authors.

Published on Web 07/15/2010

Table 1. Formulations, Particle Sizes, and PDIs for All Experiments[a]

run	initiator/mass (g)	monomers/mass (g)	CoTFB (mol %)[b]	water (g)	particle size (nm)	PDI
1	APS/0.021	NIPAM/0.5 MBA/0.1	22.6	1.0	177	0.043
2	AIBN/0.015	NIPAM/0.5 MBA/0.025	11.3	1.0	235	0.157
3	AIBN/0.015	NIPAM/0.5 MBA/0.025	22.6	1.0	252	0.060
4	AIBN/0.015	NIPAM/0.5 MBA/0.025	45.2	1.0	204	0.041
5	APS/0.021	NIPAM/0.5 MBA/0.025	22.6	1.0	245	0.032
6	APS/0.021	NIPAM/0.5 MBA/0	22.6	1.0	288	0.106
7	APS/0.021	NIPAM/0.5 MBA/0	45.2	1.0	233	0.092
8	APS/0.021	NIPAM/0.5 MBA/0.05	22.6	1.0	204	0.057
9	APS/0.021	NIPAM/0.5 MBA/0.075	22.6	1.0	173	0.037
10	APS/0.021	NIPAM/0.5 MBA/0.075	22.6	0.5	159	0.058
11	APS/0.021	NIPAM/0.5 MBA/0.075	22.6	1.5	164	0.052
12	APS/0.021	NIPAM/1.0 MBA/0.15	22.6	1	165	0.086
13	APS/0.021	NIPAM/2.0 MBA/0.30	22.6	1	175	0.053

[a] The mass of CH used in all runs was 12.5 g. [b] On the basis of the molar amount of NIPAM.

nanocapsules. In the present work, narrowly size-distributed cross-linked PNIPAM nanocapsules were synthesized via the polymerization of NIPAM and MBA in inverse miniemulsion. To our best knowledge, this is the first time for preparation of nanocapsules in inverse miniemulsion by following a phase separation mechanism simply under thermodynamic control.

Experimental Section

Materials. The monomer, *N*-isopropylacrylamide (NIPAM, Acros, 97.0%) and the cross-linking agent *N*, *N*′-methylene bis(acrylamide) (MBA, Merck, 98.0%) were used as received. The block copolymer surfactant, poly(ethylene-*co*-butylene)-*b*-poly(ethylene oxide) (P(E/B)−PEO), was synthesized according to the literature.[27,28] The molecular weight of P(E/B)−PEO used was 6200 g mol^{-1} determined by ^{1}H NMR. The constant block length of the hydrophobic block (4000 g mol^{-1}) gives an HLB value (hydrophilic−lipophilic balance) of 7.[29] The initiators ammonium persulfate (APS, Merck, 98.0%) and α,α′-azobis-(isobutyronitrile) (AIBN, Merck, 98.0%), the apolar solvent cyclohexane (CH, 99.5%, VWR Prolabo), and the metal salt cobalt(II) tetrafluoroborate hexahydrate (CoTFB, Aldrich, 99.0%) were used as received. Demineralized water with Milli-Q grade (resistivity is 18 MΩ) was used.

The Preparation of Inverse Miniemulsion and Polymerization. A 3 wt % sample of surfactant P(E/B)−PEO with respect to the polar mixture was dissolved in 12.5 g of CH under magnetic stirring. CoTFB and monomers were first dissolved in water to form homogeneous polar solutions. The polar phase was mixed with the surfactant solution. After 15 min pre-emulsification under strong magnetic stirring, the mixture was treated with 120 s ultrasound with a Branson 450 W digital sonifier at 90% amplitude in an ice bath to prepare a miniemulsion. The initial miniemulsion was introduced to the reactor, and purged with argon for 3 min under magnetic stirring. The argon protected reaction mixture was placed in a preheated oil bath at 65 °C and stirred for 5 h. The respective amounts and detailed conditions are given in Table 1.

The Preparation of Aqueous Dispersions of Nanocapsules. The original dispersion was redispersed in water according to the following protocol. About 0.5 g of the original dispersion was added to a solution of 45 mg SDS in 15 g of water. Then the mixture was strongly agitated for 30 min, followed by 2 min ultrasonification with 70% amplitude in an ice bath. The aqueous dispersion was poured into an open glass bottle and stirred at room temperature for more than 2 days to remove CH. The aqueous dispersion was used to characterize the thermosensitivity of PNIPAM nanocapsules in water.

Characterization. *Dynamic Light Scattering*. The size and size distribution (as PDI) in CH dispersion were measured by DLS (Nano-Zetasizer, Malvern Instruments) at 20 °C under the scattering angle of 173° at a wavelength of 633 nm. The original dispersions were diluted with CH in a glass cuvette before the measurement. Particle sizes and PDIs are given as the average of five measurements. The PDI is a measure of the particle size distribution and the PDI is a dimensionless number that describes the heterogeneity of the sample; it can range from 0 (monodisperse) to 1 (polydisperse).

Transmission Electron Microscopy (*TEM*). TEM measurements were performed on a Philips EM 400 Microscope. 1.5 μL of dispersion was diluted with 3 mL of CH, and then 2.0 μL of the diluted sample was placed on a 400-mesh carbon-coated copper grid and dried at room temperature overnight.

Atomic Force Microscopy (*AFM*). The original dispersions were diluted with the 3-fold amount of CH, and the diluted dispersions were cast onto cleaved mica by spin coating. AFM images (height and phase images) were recorded at a scanning rate of 0.5 Hz on a Nanoscope IIIa from Digital Instruments operating in the tapping mode by using a NCH cantilever (Nano world) with a spring constant of about 42 N/m and resonance frequency of about 300 kHz.

Results and Discussion

Synthesis of Narrowly Size-Distributed PNIPAM Nanocapsules. The syntheses of PNIPAM nanocapsules were performed as radical copolymerization of NIPAM and the cross-linking agent MBA initiated by APS or AIBN at 65 °C in inverse miniemulsion. The continuous phase was composed of cyclohexane (CH) and a block copolymer surfactant, namely poly(ethylene-*co*-butylene)-*b*-poly(ethylene oxide) (P(E/B)−PEO). In addition to the monomers and the initiator, a large amount of water and CoTFB was added to the dispersed phase to work as a soft template. Because of the presence of the bulky isopropyl group in the NIPAM molecule, the solubility of NIPAM in pure water differs substantially from that of the unsubstituted parent compound acrylamide. In pure water the solubility of NIPAM is around 30 wt % whereas even 2 g of NIPAM can be easily dissolved in the aqueous solution of 0.34 g of CoTFB in 1 g of water to form a transparent solution. We attribute the enhancement of NIPAM solubility in the CoTFB solution to the formation of a complex between NIPAM and CoTFB, similar to the formation of acrylamide/metal salt complexes as reported by Dzhardimalieva et al.[30] A further support for the formation of a NIPAM/CoTFB complex is the change of color from dark red (CoTFB) to purple (NIPAM/CoTFB complex). It should be pointed out that water molecules might also participate in the formation of the complex. The increase of solubility of NIPAM in the aqueous solution of CoTFB definitely provides more flexibility to design the recipes for synthesizing PNIPAM nanocapsules. In addition, the enhanced solubility of the monomer in the polar mixture shall have a positive influence on narrowing the particle size distribution as reported by Kobitskaya et al.[26]

As a case study, the product of run 1 was fully characterized to reveal the size (*Z*-average), size distribution (PDI),

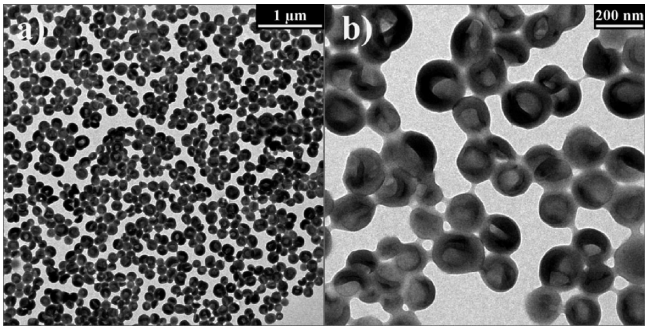

Figure 1. TEM images of cobalt salt containing PNIPAM nanocapsules synthesized in inverse miniemulsion with different magnifications (see Table 1, run 1).

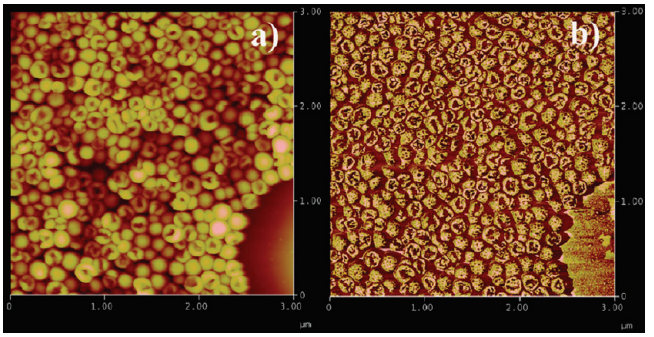

Figure 2. AFM images of PNIPAM nanocapsules synthesized in inverse miniemulsion (a, height image; b, phase image; see Table 1, run 1).

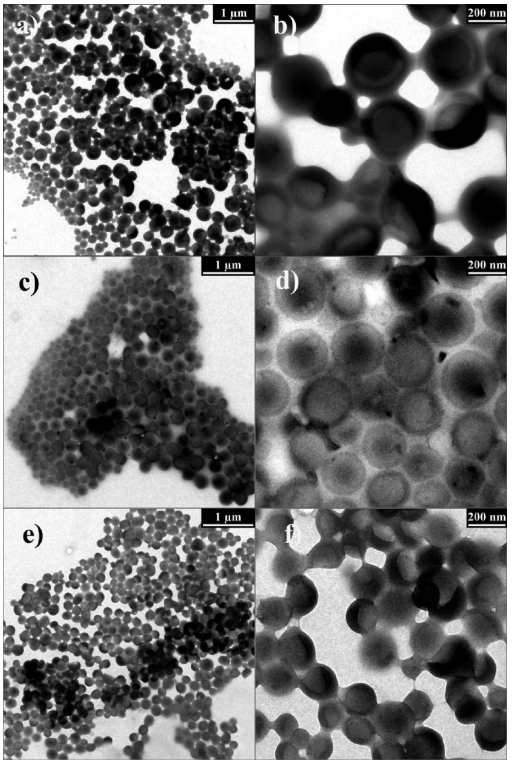

Figure 3. TEM images of PNIPAM nanocapsules synthesized in inverse miniemulsion with different contents of CoTFB (a and b, 11.3 mol % of CoTFB to NIPAM; c and d, 22.6 mol %; e and f, 45.2 mol %; see Table 1, runs 2−4).

and morphology of the particles by DLS, TEM, and AFM. The *Z*-average size and PDI of the PNIPAM particles in CH were about 177 nm and 0.043, respectively. In order to further prove the particle size distribution and reveal the detailed morphology of the particles TEM was performed (see Figure 1). The diameter of the majority of particles was in the range 160−180 nm in agreement with the DLS results. Both measurements indicate a relatively narrow particle size distribution. Concerning the morphology, the image in Figure 1b clearly displays the presence of nanocapsules with relatively thick shells. The morphology of nanocapsules was further proven by AFM (Figure 2). Indentations in nearly all particles can be observed in both the height (Figure 2a) and phase images (Figure 2b). In addition, a relatively rough surface of PNIPAM nanocapsules was revealed by the phase image (Figure 2b), similar to the observation of solid PNIPAM particles reported in literature.[31] The analogy of the experimental design between Horecha's investigations and our experiments suggests that the formation mechanism of the nanocapsules is similar.[12] Although we did not apply any additional techniques like interfacial polycondensation[20] or interfacially confined RAFT polymerization[23] to restrict the reactions to the interface between the dispersed and continuous phases, we still suppose that the polymerization took place preferentially at the interface under thermodynamic control. The thermodynamically favorable morphology of an immiscible tertiary system depends on the interfacial tensions of the different phases.[32] The interfacial tensions of PNIPAM/oil and PNIPAM/aqueous solution of CoTFB are most probably lower than that of CH/aqueous solution of CoTFB due to the amphiphilic properties of PNIPAM, similar to the case reported by Horecha et al..[12] Thus, there is a high probability for the PNIPAM molecules to diffuse and accumulate at the interface of oil/water to lower the Gibbs free energy of the system by the formation of PNIPAM/CH and PNIPAM/aqueous solution of CoTFB interface. This is the first time by simply taking advantage of the phase separation mechanism to prepare nanocapsules in inverse miniemulsion. The introduction of CoTFB was expected to be more favorable to form nanocapsules due to the increasing interfacial tension between oil and the polar mixture with the increase of CoTFB content[25] and the interaction between PNIPAM and CoTFB indicated by the purple color of the final dried product. In addition, we assume that the PNIPAM oligomeric radicals diffused to the interface before they fully propagated and phase separated in the whole droplets because of the use of APS as initiator and the introduction of a large amount of cross-linker (20 wt % of MBA to NIPAM) in the present case. Otherwise, the nanocapsules might not form due to the reduction of the mobility of polymer chains as a result of the formation of a highly cross-linked structure. The PNIPAM oligomeric radicals at the interface continuously propagated with NIPAM and MBA, and finally underwent a phase separation to form a cross-linked shell on the hydrophilic cores.

Variables Influencing the Particle Morphology and Particle Size Distribution. *Content of CoTFB.* In inverse miniemulsion, the particle size distribution is sensitive to the variation of the metal salt content.[25,26] We carried out the polymerizations in the systems containing 11.3−45.2 mol % of CoTFB with respect to NIPAM with AIBN as initiator (see Table 1, run 2−4). Only a broad particle size distribution could be obtained with 11.3 mol % of CoTFB according to the results of DLS (PDI = 0.157) and TEM (see Figure 3a). Some small solid particles can be found in Figure 3a. Although the solubility of NIPAM in the oil phase at room temperature is negligible, it significantly increases to 20% when the temperature increases to 80 °C.[12] Despite the presence of the

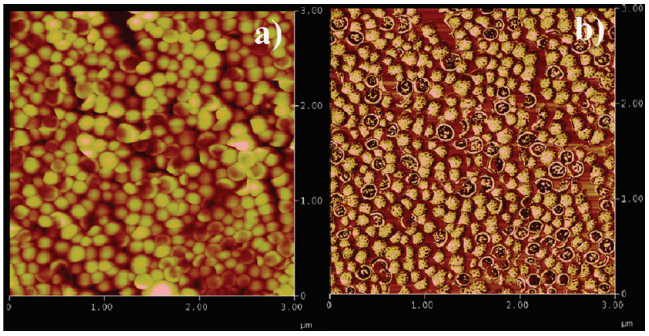

Figure 4. AFM images of PNIPAM nanocapsules synthesized in inverse miniemulsion with 45.2 mol % of CoTFB initiated by AIBN (a, height image; b, phase image; see Table 1, run 4).

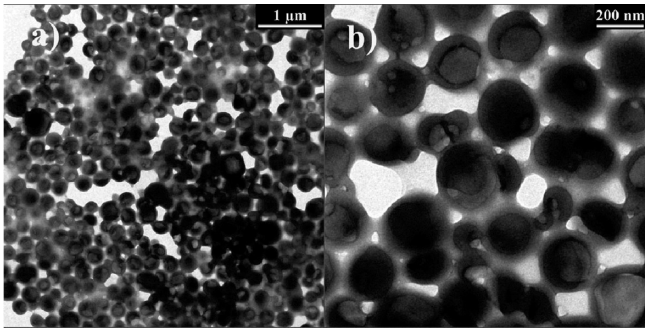

Figure 5. TEM images of PNIPAM nanocapsules synthesized in inverse miniemulsion by using APS as initiator (see Table 1, run 5).

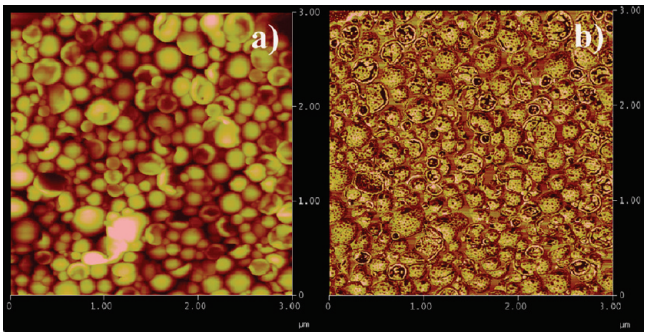

Figure 6. AFM images of PNIPAM nanocapsules synthesized in inverse miniemulsion initiated by APS (a, height image; b, phase image; see Table 1, run 5).

osmotic pressure agent in the inverse miniemulsion (lipophobe CoTFB), a certain amount of NIPAM molecules can not be ruled out in the nonpolar continuous phase. Thus, the broad particle size distribution is attributed to the poor droplet stability caused by molecular diffusion of NIPAM. In addition, the initiation locus in the present system was in the continuous phase because of the oil soluble initiator AIBN. The formation of the small solid particles is attributed to homogeneous nucleation. Most of the large "particles" display a nanocapsule morphology (Figure 3 right). As described in our previous paper,[25] the droplet stability could be effectively improved by increasing the amount of metal salt in the inverse miniemulsion. A corresponding dependence could be shown for the present system, and the particle size distributions indicated by the PDI were significantly reduced from 0.157 to 0.041 with the increase of the CoTFB content from 11.3 mol % to 45.2 mol % to NIPAM. In addition, the small particles were also significantly decreased in number and could hardly be detected for the system with 45.2 mol % of CoTFB. The suppression of homogeneous nucleation is ascribed to the decrease of the concentration of NIPAM in the continuous phase due to the increase of droplet stability as the result of the increased amount of CoTFB. The morphology of the nanocapsules formed can be observed in TEM with high magnification (Figure 3, parts d and f). Most of the particulate objects containing 45.2 mol % of CoTFB display indentations as confirmed by AFM (Figure 4a,b).

Initiator Types. As discussed before, the initiation locus in the continuous phase is one possible reason for undesirable homogeneous nucleation. It can be easily shifted from the continuous phase to the dispersed phase by using water-soluble initiators like ammonium persulfate (APS) in inverse miniemulsion system. Expectedly, the amount of small solid particles in the system initiated by APS (run 5) is significantly reduced compared to the system with AIBN as initiator (run 3 and Figure 5a). However, in contrast to the low PDI (0.032), a relatively broad particle size distribution is shown by TEM (Figure 5a) and AFM (Figure 6a and 6b). Nearly all initial droplets were successfully transformed to nanocapsules during polymerization (Figure 5 and Figure 6). The indentation can be observed not only on the large but also on the relatively small particles. Thus, homogeneous nucleation can be mainly ruled out. These results support that the polymerization took place essentially at the interface between the continuous and dispersed phase. The initiation was mainly located in the droplets when APS was employed as initiator. If the reaction would have happened in the whole droplet, the polymer chains might have become too rigid because of the presence of cross-linker (MBA), thus, rather leading to a homogeneous solid morphology than to nanocapsules.

Amount of MBA. Cross-linkers not only help to construct stable nanocapsules, but can also significantly affect the morphology of particles. A series of experiments was carried out to investigate the dependence of particle morphology on the amount of MBA (see Table 1, run 1 and 5−9). We have shown that the latex particles generated by droplet nucleation could finally form nanocapsules and the fraction of nanocapsules was not deteriorated by the presence of 20 wt % of the cross-linker MBA to NIPAM. On the contrary, some small solid particles appeared in the system without addition of MBA and the particle size distribution broadened (see in Figure 7a and Figure 8). In order to reduce the amount of solid particles, which were formed presumably by homogeneous nucleation (see above) and improve the particle size distribution, the CoTFB content was increased to 45.2 mol % to NIPAM. However, this increase had only a minor influence on the particle size distribution (see TEM image in Supporting Information, Figure S1). Instead, the particle size distribution could be significantly narrowed by the addition of MBA and further improved by the increase of its amount. With a relatively high content of MBA the small solid particles even disappeared in the system. Therefore, we believe that the amount of cross-linker is one of the important parameters to influence the particle size distribution and homogeneous nucleation. Furthermore, the size of nanocapsules decreased from 288 nm to about 170 nm with the increase of MBA from 0 to 15 wt % to NIPAM, and then remained constant until the MBA content increased to 20 wt % (see Figure S2). Comparing the AFM images of samples with different MBA amount shows that most of the un-cross-linked nanocapsules collapsed forming oblate objects as shown by AFM (Figure 8), while the cross-linked nanocapsules

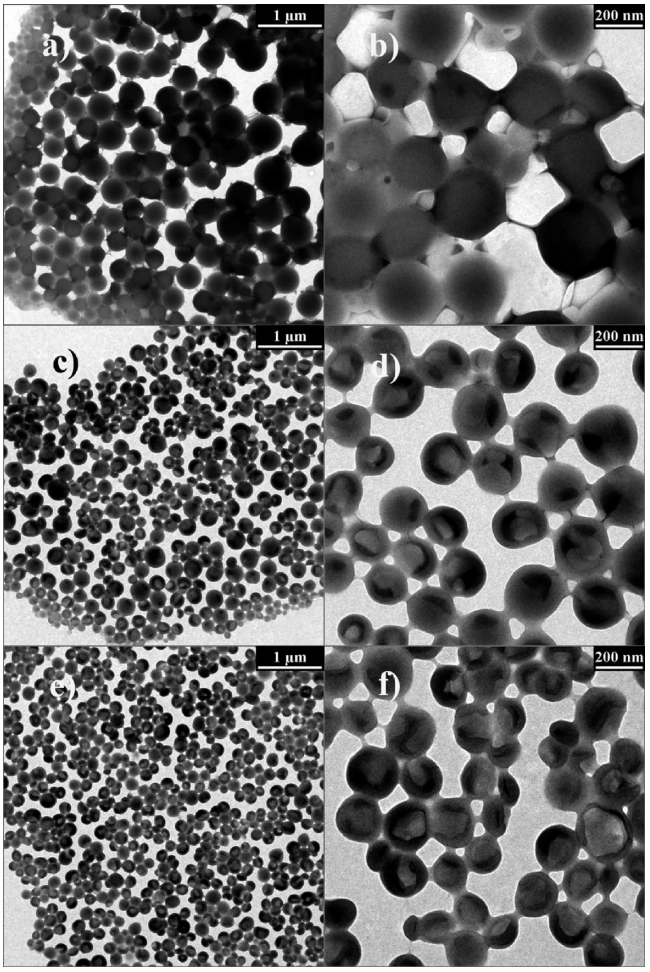

Figure 7. TEM images of PNIPAM nanocapsules synthesized in inverse miniemulsion by using different contents of MBA (a and b, 0 wt % of MBA to NIPAM; c and d, 10 wt %; e and f, 15 wt %; see Table 1, run 6, 8, and 9).

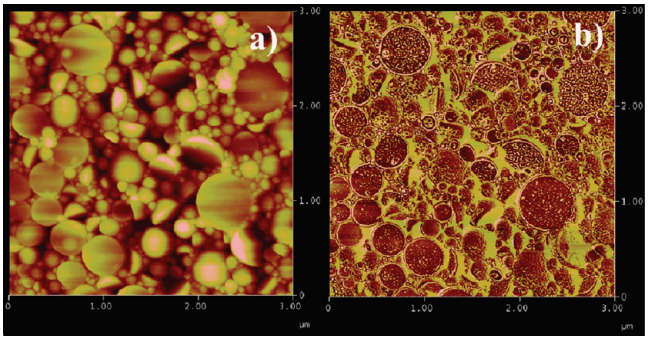

Figure 8. AFM images of PNIPAM nanocapsules synthesized in inverse miniemulsion without addition of MBA (a, height image; b, phase image; see Table 1, run 6).

collapsed forming bowl-like shapes (Figure 2, 4, and 6). This is attributed to the stabilization of the shell of the nanocapsules with increasing MBA amount due to the increase of the cross-linking extent of the shell copolymers. The different three-dimensional shapes of the nanocapsules after drying can also explain why the contrast in Figure 7, parts a and b, does not show unambigously a nanocapsule morphology contrary to the systems with addition of cross-linker.

Content of Water and Monomer. A broad particle size distribution was observed in the system with only 100 wt % of water to NIPAM (see Table 1, run 10 and Figure 9a). Not only small but also solid particles without capsule morphology are found (Figure 9, parts a and b) pointing to homogeneous nucleation (see above). This is ascribed on one side to the decrease of interfacial tension with decreasing water content and thus lowered driving force for the oligomer and polymer chains to approach the interface. On the other side an increase of viscosity of the liquid phase with reduced water content decreases the mobility of the chains. Once the chains are cross-linked in the interior of the latex particles, the initial droplets finally form solid particles. The increase of water content caused a higher droplet stability, narrowed the particle size distribution and reduced the amount of small solid particles produced by homogeneous nucleation (see Table 1, run 9 and 11, Figure 7e and 9c). Nearly all droplets formed nanocapsules in the systems with 200 and 300 wt % of water to NIPAM (Figure 7e, 7f, 9c, and 9d).

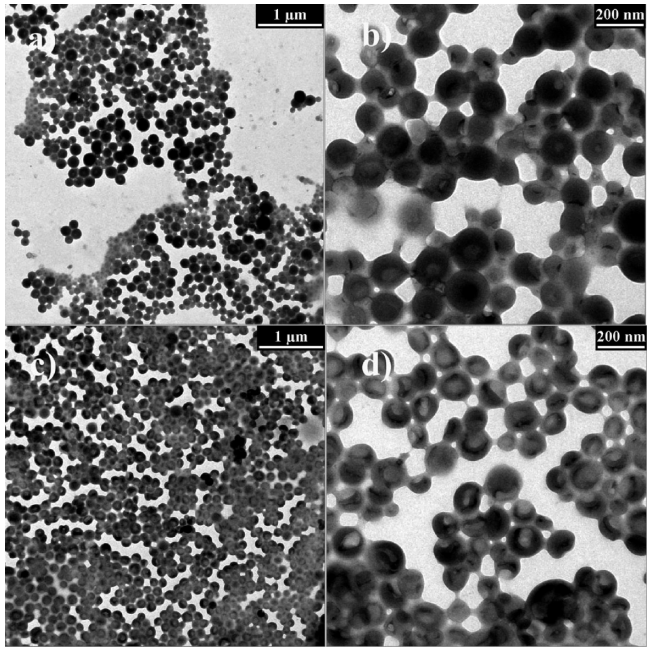

Figure 9. TEM images of PNIPAM nanocapsules synthesized in inverse miniemulsion by using different water contents (a and b, 100 wt % of water to NIPAM; c and d, 300 wt % of water to NIPAM; see Table 1, run 10 and 11).

Correspondingly to the results of run 9 with 50 wt % NIPAM to water, the increase of the monomer content to 100 and 200 wt % of NIPAM to a fixed amount of water (see Table 1, run 12 and 13) led to the formation of solid particles as shown in Figure 10.

Discussion on Homogeneous Nucleation. In most cases, the formation of solid particles is caused by homogeneous nucleation. Homogeneous nucleation is determined by the generation rate of oligomeric chains in the continuous phase and the adsorption and desorption rate of oligomeric chains by droplets or latex particles.[33,34] A high generation rate and slow adsorption rate of oligomeric chains are favorable for homogeneous nucleation. The generation rate of oligomeric chains in the continuous phase can be reduced by decreasing the concentration of primary and monomer radicals, and monomers in the continuous phase. Both the improvement of droplet stability to suppress the molecular diffusion and initiating the polymerization in the dispersed phase by applying a water-soluble initiator are favorable to reduce homogeneous nucleation. This is supported by the fact that the amount of small solid particles decreased with the increase

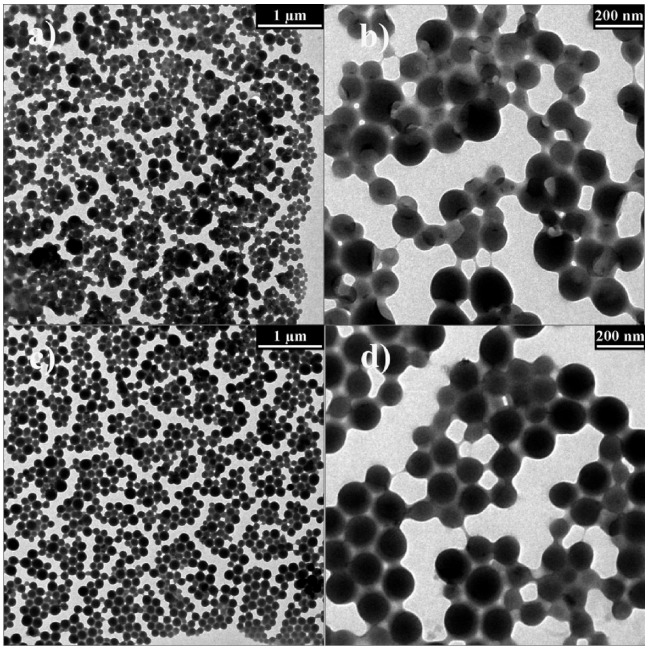

Figure 10. TEM images of PNIPAM nanocapsules synthesized in inverse miniemulsion by using different NIPAM amounts (a and b, 100 wt % of NIPAM to water; c and d, 200 wt % of NIPAM to water; see Table 1, run12 and 13).

of CoTFB and water content, or using APS as initiator as shown before. The increase of the amount of MBA also had a positive influence on the suppression of homogeneous nucleation. We assume that the enhancement of cross-links in the shell may reduce the desorption rate of monomeric radicals from the latex particles, resulting in a decrease of concentration of radicals in the continuous phase. Here, it is necessary to point out that the homogeneous nucleation is not the only reason for the formation of solid particles. In fact, the polymerization taking place in the droplets also leads to the formation of solid particles when the thermodynamic driving force is insufficient to compel the oligomers or polymer chains to approach the interface, such as in the cases with a high ratio between NIPAM and water. In literature, a peculiar formation mechanism for solid particles in a heterophase system is described based on complete phase separation of polymer within a vesicle bilayer membrane probably due to unfavorable polymer−surfactant interaction and restricted conformational freedom.[35,36] In order to avoid the intravesicular phase separation, another technique, so-called polymerization of vesicles, was adopted by using polymerizable amphiphiles.[37] Instead of the formation of solid particles, the stability of vesicles can be in fact improved by the polymerization of vesicles, especially in the case by the application of cross-linking amphiphiles the intravesicular phase separation can be avoided and produce a stable network.[37] However, in our case, the phase separation of polymer from the aqueous solution of salt is the prerequisite to prepare nanocapsules (according to the observed results, polymer phase separation mainly happens at the interface). In fact, the system without phase separation such as by using acrylamide to replace NIPAM or carrying out the reaction at a temperature below the LCST of NIPAM only produces solid particles due to the reaction taking place in the whole particle.[12] Therefore, we believe the mechanism to control particles' morphology in the case of polymerization in or of vesicles can be ruled out for the present systems.

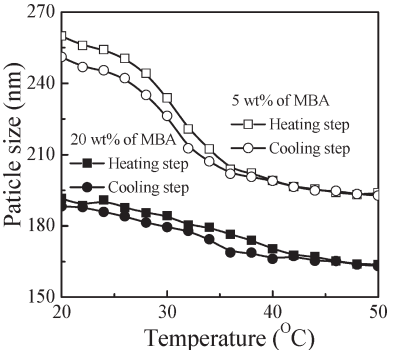

Figure 11. Dependence of size of PNIPAM nanocapsules in water on temperature (see Table 1, run 1 and 5).

Table 2. Dependence of the Size of Nanocapsules Dispersed in CH on Temperature

	particle size (nm)			
	run 1 (Table 1)		run 5 (Table 1)	
temperature (°C)	heating	cooling	heating	cooling
20	177	165	245	230
30	167	166	234	217
40	159	168	215	201
50	167	167	198	198

Thermosensitive Properties of Nanocapsules. Because of the swelling of the PNIPAM shell by water, the sizes of the nanocapsules redispersed in water were always larger than those dispersed in CH regardless of the MBA content. The nanocapsules showed an obvious temperature dependent volume phase transition (Figure 11). With the increase of the temperature from 20 to 50 °C, the size of nanocapsules decreased from 260 to 194 nm for the product synthesized with 5 wt % of MBA (run 5) due to the continuous deswelling of the PNIPAM shell. The decrease of particle size from 192 to 164 nm for the system with 20 wt % of MBA (run 1) is less visible what is ascribed to the more cross-linked shell, confining the response of volume transition to the temperature variation. The most pronounced change in the size of the nanocapsules of run 5 took place in the temperature range from 24 to 36 °C, with about 31 °C at the half step height, close to the LCST of PNIPAM reported in literature (32 °C).[9,38] The nanocapsules of run 1 showed a relatively slow response to the temperature change, and the particle size gradually decreased in the range from 26 to 42 °C. The slow response is again attributed to the highly cross-linked structure. In addition, the temperature at the half step height increased (36.7 °C) compared to run 5. The swelling and deswelling of the PNIPAM shell are reversible.

The size variation with the change of temperature of PNIPAM nanocapsules dispersed in CH was also investigated in the range of 20 to 50 °C. According to the results in Table 2, with increasing temperature, the sizes of PNIPAM nanocapsules with 5 and 20 wt % of MBA decreased. The sizes of nanocapsules dispersed in CH at 50 °C were close to the size of nanocapsules dispersed in water at the same temperature. This means that the PNIPAM nanocapsules dispersed in CH also can undergo a complete collapse at 50 °C similar to the nanocapsules dispersed in water. Considering the highly diluted dispersion for DLS measurement and a relatively higher solubility of water in CH at an elevated temperature (0.012 and 0.049 wt % at 20 and 50 °C),[39] the small amount of water inside the PNIPAM nanocapsules is expected to dissolve in CH. Unlike the PNIPAM nanocapsules dispersed in water, the PNIPAM nanocapsules with

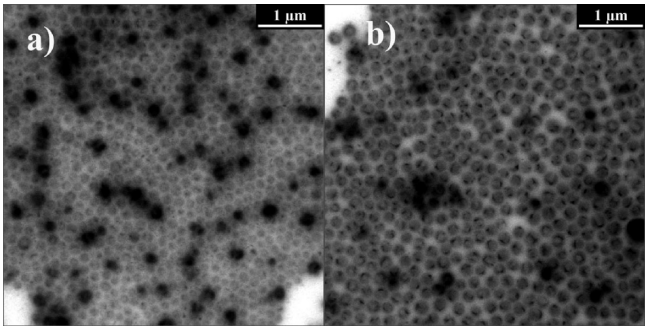

Figure 12. TEM images of PNIPAM nanocapsules dispersed in isopar M. (a, dried at 50 °C; b, dried at room temperature; see Table 1, run 1).

20 wt % of MBA (run 1) could not be reswollen by water indicated by an unchanged particle size with decreasing temperature. The PNIPAM nanocapsules with 5 wt % of MBA (run 5) could be reswollen by water to some extent, though the final size (230 nm) at 20 °C was lower than the initial particle size (245 nm). Rationally, the swelling of the highly cross-linked PNIPAM shell and the diffusion of water through this shell into the nanocapsules are kinetically more difficult compared to a weakly cross-linked shell. In addition, the low driving force to reswell the PNIPAM shell in CH due to only a small amount of water present in the diluted CH dispersion might be partially responsible for the loss of reversible thermosensitivity.

Formation of Monolayers of PNIPAM Nanocapsules. The evaporation rate of apolar solvent in the continuous phase is critical to form ordered arrays of particles. In contrast to the arrays of particles dispersed in CH, better ordered arrays of PNIPAM nanocapsules were obtained by using isopar M as the apolar solvent due to its lower evaporation rate than that of CH (Figure 12). Taking advantage of the volume phase transition of PNIPAM below and above its LCST, the particle size of PNIPAM nanocapsules could be possibly tuned by changing the drying temperatures. Roughly estimated from the TEM images dried under room temperature (below LCST) and 50 °C (above LCST), the average diameters of PNIPAM nanocapsules (run 9) dried at room temperature were about 30 to 50 nm larger than those of PNIPAM nanocapsules dried at 50 °C derived from the Fourier transform of the TEM images (see Supporting Information, Figure S3). This value was fairly in agreement with the size variation of nanocapsules dispersed in water (28 nm), higher than that of nanocapsules dispersed in CH (10 nm). It provides the possibility to directly vary the periodicity of ordered particulate arrays with the same sample only by temperature variation without need for additional growth of particle size by seeded emulsion polymerization as reported previously.[24]

Conclusion

Narrowly size-distributed thermosensitive poly(*N*-isopropylacrylamide) PNIPAM nanocapsules with a hydrophilic core were successfully synthesized via the one-pot inverse miniemulsion polymerization of *N*-isopropylacrylamide (NIPAM). The solubility of NIPAM was significantly improved by using cobalt tetrafluoroborate (CoTFB) which worked as template and lipophobe as well. The polymerization took place favorably at the interface of the dispersed and continuous phase in the system with 50 wt % of NIPAM to water concluded from the nanocapsule morphology of the resulting nanoobjects with both water- and oil-soluble initiators in the presence of cross-linker (MBA). The increase of amount of cross-linker with the water-soluble initiator increased the morphological stability of the nanocapsules. Both the reduction of water amount and the increase of NIPAM amount to increase the ratio of NIPAM and water led to the loss of the nanocapsule morphology of the particles formed by droplet nucleation. The particle size distribution could be effectively narrowed by the increase of CoTFB content, MBA amount, and water content in the experimental range. Solid particles appearing in some systems were produced by homogeneous nucleation due to the relatively high solubility of NIPAM in the continuous phase. The homogeneous nucleation could be suppressed by increasing the droplet stability (using more CoTFB, water or MBA) or reducing the concentration of radicals in the continuous phase (using water-soluble initiator). The thermosensitivity of as-prepared PNIPAM nanocapsules was confirmed by the obvious shrinkage of the nanocapsules indicated by the decrease of particle size when increasing the temperature from 20 to 50 °C. The PNIPAM nanocapsules could form ordered monolayers by using isopar M to dilute the original CH dispersion, and the difference in size of the nanocapsules for the same sample was about 30−50 nm when drying at room temperature and at 50 °C. Further work is dedicated to improving the order of the arrays and controlling the packing density.

Acknowledgment. We greatly thank Dr. C. Hoffmann-Richter for the AFM measurements and G. Weber for the synthesis of P(E/B)−PEO. The support by Deutsche Forschungsgemeinschaft (DFG) within the Cooperative Research Center SFB 569 is gratefully acknowledged.

Supporting Information Available: Figures showing additional TEM images and graphs. This material is available free of charge via the Internet at http://pubs.acs.org.

References and Notes

(1) Landfester, K. *Angew. Chem., Int. Ed.* **2009**, *48*, 4488–4507.
(2) Zhu, A.; Pan, Y.; Dai, S.; Li, F.; Shen, J. *Biomacromolecules* **2009**, *10*, 1997–2002.
(3) Xie, L.; Chem, M.; Wu, L. *J. Polym. Sci., Part A: Polym. Chem.* **2009**, *47*, 4919–4926.
(4) Torchilin, V. *Eur. J. Pharm. Biopharm.* **2009**, *71*, 431–444.
(5) Gao, H.; Yang, W.; Min, K.; Zha, L.; Wang, C.; Fu, S. *Polymer* **2005**, *46*, 1087–1093.
(6) Sukhorukov, G.; Fery, A.; Möhwald, H. *Prog. Polym. Sci.* **2005**, *30*, 885–897.
(7) Stuart, M. A. C.; Huck, W. T. S.; Genzer, J.; Müller, M.; Ober, C.; Stamm, M.; Sukhorukov, G. B.; Szleifer, I.; Tsukruk, V. V.; Urban, M.; Winnik, F.; Zauscher, S.; Luzinov, I.; Minko, S. *Nature Mater.* **2010**, *9*, 101–113.
(8) Heskins, M.; Guillet, J. E. *J. Macromol. Sci., Chem.* **1969**, *2*, 1441–1455.
(9) Schild, H. G. *Prog. Polym. Sci.* **1992**, *17*, 163–249.
(10) Huang, C.-J.; Chang, F.-C. *Macromolecules* **2009**, *42*, 5155–5166.
(11) Sun, Q.; Deng, Y. *J. Am. Chem. Soc.* **2005**, *127*, 8274–8275.
(12) Horecha, M.; Senkovskyy, V.; Stamm, M.; Kiriy, A. *Macromolecules* **2009**, *42*, 5811–5817.
(13) Tiarks, F.; Landfester, K.; Antonietti, M. *Langmuir* **2001**, *17*, 908–918.
(14) Ni, K. F.; Shan, G. R.; Weng, Z. X. *Macromolecules* **2006**, *39*, 2529–2535.
(15) Cao, Z.; Shan, G. R. *J. Polym. Sci., Part A: Polym. Chem.* **2009**, *47*, 1522–1534.
(16) Cao, Z. H.; Shan, G. R.; Sheibat-Othman, N.; Putaux, J. L.; Bourgeat-Lami, E. *J. Polym. Sci., Part A: Polym. Chem.* **2010**, *48*, 593–603.
(17) Li, W.; Matyjaszewski, K.; Albrecht, K.; Möller, M. *Macromolecules* **2009**, *42*, 8228–8233.
(18) van Zyl, A. J. P.; Sanderson, R. D.; Wet-Roos, D.; Klumperman, B. *Macromolecules* **2003**, *36*, 8621–8629.
(19) Luo, Y. W.; Gu, H. Y. *Macromol. Rapid Commun.* **2006**, *27*, 21–25.
(20) Crespy, D.; Stark, M.; Hoffmann-Richter, C.; Ziener, U.; Landfester, K. *Macromolecules* **2007**, *40*, 3122–3135.
(21) Rosenbauer, E.-M.; Landfester, K.; Musyanovych, A. *Langmuir* **2009**, *25*, 12084–12091.

(22) Paiphansiri, U.; Dausend, J.; Musyanovych, A.; Mailander, V.; Landfester, K. *Macromol. Biosci.* **2009**, *9*, 575–584.
(23) Lu, F.; Luo, Y.; Li, B.; Zhao, Q.; Schork, F. J. *Macromolecules* **2010**, *43*, 568–571.
(24) Schreiber, E.; Ziener, U.; Manzke, A.; Plettl, A.; Ziemann, P.; Landfester, K. *Chem. Mater.* **2009**, *21*, 1750–1760.
(25) Cao, Z.; Wang, Z.; Herrmann, C.; Ziener, U.; Landfester, K. *Langmuir* **2010**, *26*, 7054–7061.
(26) Kobitskaya, E.; Ekinci, D.; Manzke, A.; Plettl, A.; Ziemann, P.; Ziener, U.; Landfester, K. *Macromolecules* **2010**, *43*, 3294–3305.
(27) Schlaad, H.; Kukula, H.; Runloff, J.; Below, I. *Macromolecules* **2001**, *34*, 4302–4304.
(28) Thomas, A.; Schlaad, H.; Smarsly, B.; Antonietti, M. *Langmuir* **2003**, *19*, 4455–4459.
(29) Rosen, M. J. *Surfactants and interfacial phenomena*; Wiley: New York, 1978; p 304.
(30) Dzhardimalieva, G. I.; Pomogailo, A. D.; Volpert, V. A. *J. Inorg. Organomet. Polym.* **2002**, *12*, 1–21.
(31) Kratz, K.; Hellweg, T.; Eimer, W. *Polymer* **2001**, *42*, 6631–6639.
(32) Torza, S.; Mason, S. G. *J. Colloid Interface Sci.* **1970**, *33*, 67–83.
(33) Fitch, R. M.; Tsai, C. H. *Polymer colloids*; Plenum Press: New York, 1971; p 73.
(34) Fitch, R. M.; Tsai, C. H. *Polymer colloids*; Plenum Press: New York, 1971; p 103.
(35) Jung, M.; Hubert, D. H. W.; Bomans, P. H. H.; Frederik, P. M.; Meuldijk, J.; van Herk, A. M.; Fischer, H.; German, A. L. *Langmuir* **1997**, *13*, 6877–6880.
(36) Jung, M.; Hubert, D. H. W.; van Veldhoven, E.; Frederik, P.; van Herk, A. M.; German, A. L. *Langmuir* **2000**, *16*, 3165–3174.
(37) Jung, M.; den Ouden, I.; Montoya-Goñi, A.; Hubert, D. H. W.; Frederik, P. M.; van Herk, A. M.; German, A. L. *Langmuir* **2000**, *16*, 4185–4195.
(38) Pelton, R. H.; Pelton, H. M.; Morphesis, A.; Rowell, R. L. *Langmuir* **1989**, *5*, 816–818.
(39) Énglin, B. A.; Platé, A. F.; Tugolukov, V. M.; Pryanishnikova, M. A. *Chem. Tech. Fuels Oils* **1965**, *1*, 722–726.